Journal of Alloys and Compounds 521 (2012) 45–49

Contents lists available at SciVerse ScienceDirect

Journal of Alloys and Compounds

journal homepage: www.elsevier.com/locate/jallcom

Synthesis and characterization of $La_{0.6}Sr_{0.4-x}Ca_xCo_{0.2}Fe_{0.8}O_3$ materials by the gel-casting process

Jigui Cheng[a,*], Jie Dong[a], Qiumei Jiang[a], Rui Wang[a], Jianfeng Gao[b]

[a] School of Materials Science and Engineering, Hefei University of Technology, Hefei 230009, China
[b] Department of Materials and Engineering, University of Science of China, Hefei 230022, China

ARTICLE INFO

Article history:
Received 22 April 2009
Received in revised form
31 December 2011
Accepted 3 January 2012
Available online 25 January 2012

Keywords:
$La_{0.6}Sr_{0.4-x}Ca_xCo_{0.2}Fe_{0.8}O_3$ ceramics
Gel-casting
Perovskite structure
Cathode material
Thermal expansion coefficient (TEC)

ABSTRACT

$La_{0.6}Sr_{0.4-x}Ca_xCo_{0.2}Fe_{0.8}O_3$ (LSCCF) powders were prepared from relative oxides and carbonate powders by a gel-casting process. Phase structure of the obtained powders with different calcium dosages ($x = 0.0$, 0.2, 0.4) was investigated. Density and porosity of the sintered LSCCF samples were measured by the Archimedes method. Microstructure was observed by scanning electron microscope (SEM) and electrical conductivity of the specimens was tested using the four-probe method. Effects of calcium dosage on the thermal expansion coefficient (TEC) of the sintered LSCCF samples were also studied. The results showed that superfine and well-dispersed LSCCF powders with perovskite structure were obtained when the dried gels were calcined at temperature above 1000 °C. The calcium dosage and sintering temperature have an obvious influence on the density and pore characteristics of the LSCCF samples. Open porosities of LSCCF samples sintered at different temperature vary from 4.7% to 50.2%, decreasing as calcium dosage and sintering temperature increase. Thermal expansion coefficients of the LSCCF materials also greatly depend on calcium dosage. A typical TEC value of $13.05 \times 10^{-6}\ K^{-1}$ for $La_{0.6}Sr_{0.2}Ca_{0.2}Co_{0.2}Fe_{0.8}O_3$ samples was obtained at 800 °C, lower than values obtained for samples with no calcium dosage. Electrical conductivity of the LSCCF samples decreases as calcium dosage increases, but all samples showed a conductivity value above 300 S cm^{-1} at 400–800 °C, which can satisfy the requirements of cathode materials for solid oxide fuel cells.

1. Introduction

Solid oxide fuel cells (SOFCs) have nowadays received considerable attention due to their high electrical efficiency, environmentally friendly nature and high flexibility of fuels [1–3]. However, the conventional SOFCs have to operate at high temperatures (800–1000 °C), which may cause several problems associated with the corrosion of metal interconnect materials and the decrease of triple phase boundary (TPB) by sintering of electrode particles during long-term operation [4]. In order to overcome these drawbacks, there is an increasing interest in developing intermediate-temperature (600–800 °C) solid oxide fuel cells (IT-SOFCs) [5]. Lowering the operation temperature to intermediate-temperature rang can allow for a wide choice of cell materials, reduce the cost of SOFCs system through the use of metallic components [1,6]. Nevertheless, such low temperature necessarily leads to low cell performances because of the low ionic conductivity of electrolyte and the over potential of the electrode. In particular, cathode polarization appears to have a greater negative effect on cell performance than anode polarization for SOFCs operated at low temperature [4]. Therefore, development of new cathode materials for low temperature operation becomes a crucial issue for the practical applications of IT-SOFCs [1].

Recently $La_{1-x}Sr_xCo_{1-y}Fe_yO_{3-\delta}$ (LSCF) perovskite oxides have drawn much attention in use as cathode materials for SOFCs to replace the conventional $La_{1-x}Sr_xMnO_{3-\delta}$ (LSM) materials, because of the high catalytic activity of LSCF for oxygen reduction (about one order of magnitude higher than that of LSM) [7]. Up to now, LSCF with composition of $La_{0.6}Sr_{0.4}Co_{0.2}Fe_{0.8}O_{3-\delta}$ (LSCF6428) has been widely investigated as alternative cathode material because of its high electronic and oxygen ion conductivity as well as electrocatalytic activity [8]. Doping of strontium can efficiently improve electrical conductivity of this cathode material. However, it also causes the accretion of thermal expansion coefficient (TEC) of the material, which may result in the mismatch between the electrode and the electrolyte [9,10]. Therefore, further research has been aimed at overcoming the shortfalls associated with LSCF6428 cathode materials by partial substitution of strontium (Sr) ions with calcium (Ca) ions (smaller ionic radius) or barium (Ba) ions (larger ionic radius) to perturb the crystal structure differently for studying the effects of such a perturbation on the defect chemistry and the transport properties [11,12]. But by now, the effects of Ca dosage

* Corresponding author. Fax: +86 0551 2901793.
E-mail address: jgcheng@sina.com (J. Cheng).

0925-8388/$ – see front matter © 2012 Elsevier B.V. All rights reserved.
doi:10.1016/j.jallcom.2012.01.003

on the crystallographic characteristic, electricity conductivity and thermal property of $La_{0.6}Sr_{0.4-x}Ca_xCo_{0.2}Fe_{0.8}O_3$ material have been less studied.

Perovskite powders for SOFC cathodes are commonly synthesized by solid state reaction, and some other chemical methods such as co-precipitation method, glycine nitrate process and EDTA-citrate complexing method [5,13,14]. Recently, a new soft chemical route named gel-casting has been successfully employed to synthesize perovskite ceramic powders and porous ceramics. In the gel-casting process, insoluble or low-solubility precursors are employed to form a dense suspension, which are solidified by the polymerization of organic monomers. The homogeneous gelcasts are subsequently dried and calcined to obtain ceramic powders or sintered bodies [15]. The gel-casting method has unique advantages of simple processing, combining solid state reaction and sintering process in one step [16]. It has been shown that SOFC cathode materials with favorable microstructure and electrochemical performance can be produced by this process [17,18].

In this paper, calcium was co-doped with strontium to prepare $La_{0.6}Sr_{0.4-x}Ca_xCo_{0.2}Fe_{0.8}O_3$ (LSCCF) materials using the gel-casting process from relative oxides and carbonates, and the effects of calcium doping on the crystallographic characteristic, electrical conductivity and thermal property of the $La_{0.6}Sr_{0.4-x}Ca_xCo_{0.2}Fe_{0.8}O_3$ (LSCCF) material were investigated.

2. Experimental

2.1. Sample preparation

Analytical pure lanthana (La_2O_3), strontium carbonate ($SrCO_3$), cobalt oxide (Co_2O_3), calcium carbonate ($CaCO_3$) and iron oxide (Fe_2O_3) were used as raw materials. The chemicals, in stoichiometric ratio of $La_{0.6}Sr_{0.4-x}Ca_xCo_{0.2}Fe_{0.8}O_3$ (LSCCF, $x = 0$, 0.2, 0.4), mixed in aqueous monomers (acrylamide, AM and *N,N′*-methylenebisacrylamide, MBAM, AM:MBAM = 20:1 (wt.%) solution with a concentration of 5 wt.% of LSCCF) were ball-milled for 24 h. The resulting slurry with initiator ammonium bisulphate $(NH4)_2S_2O_8$ (about 1.5 wt.% of organic monomers) was cast into a mold and solidified by heating to a moderate temperature. The dried gels were then calcined at a temperature range from 800 °C to 1100 °C for 5 h. The obtained powders were pressed into discs of 18.5 mm in diameter and bars of 40 mm × 5 mm × 5 mm in size, followed by sintering at 1100–1250 °C for 5 h.

2.2. Characterization

Simultaneous differential thermal analysis and thermogravimetry (DTA–TG) were carried out on the dried gelcasts. Samples were heated from room temperature to 1000 °C at a heating rate of 10 °C per minute under a dynamic air flow. The gelcasts were calcined at temperature ranging from 800 °C to 1100 °C in static air for 5 h. The calcined powders with different calcium dosages were characterized by X-ray diffraction (XRD), and powder morphology was observed by transmission electron microscope (TEM). Density and porosity of the LSCCF samples sintered at different temperature were determined using the Archimedes method. Microstructure of the sintered samples was observed by scanning electron microscope (SEM). Electrical conductivity of the LSCCF samples was obtained by the four-probe method.

Average linear thermal expansion coefficients (TECs) of the sintered LSCCF samples with different calcium dosage were tested using a dilatometer (DIL 402C, Netzsch, Germany). The machined samples with 10 mm × 4.5 mm × 4.5 mm in size were heated in air from room temperature to 1000 °C at a heating rate of 5 °C/min, and relative changes of the sample length were continuously recorded.

3. Results and discussion

3.1. DTA–TG of the dried gelcasts

DTA–TG was used to analyze the thermal decomposition and phase evolvement of the $La_{0.6}Sr_{0.4-x}Ca_xCo_{0.2}Fe_{0.8}O_3$ gelcasts. Fig. 1 shows DTA–TG results of the gelcasts with $x = 0.2$. At $T < 250$ °C, there is about 10% mass loss, which may be caused by the endothermic removal of the occluded water in the polymer network of the gelcasts. In temperature range 250–450 °C, there is a big exothermic DTA peak accompanied by a large mass loss. This may be attributed to the burn-out of the cross-linked polymer networks. At 650 °C, another mass loss starts and completes at 850 °C. This

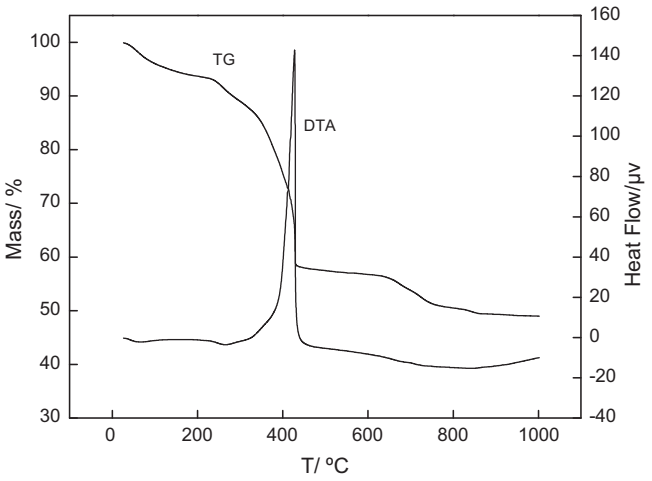

Fig. 1. DTA–TG curves of the dried gelcasts.

may be ascribed to the thermal decomposition of $SrCO_3$ and $CaCO_3$ due to solid-state reaction among the carbonates and oxides and the formation of LSCCF perovskite phase, as evidenced by XRD. No apparent mass loss occurs above 900 °C, indicating that the decomposition of the carbonates is completed.

3.2. XRD and morphology of the calcined LSCCF powders

$La_{0.6}Sr_{0.4-x}Ca_xCo_{0.2}Fe_{0.8}O_3$ gelcasts with different calcium dosages were calcined at temperature 800–1100 °C for 5 h, at an interval of 100 °C, and the products obtained were identified by XRD. Fig. 2 shows XRD patterns of the LSCCF powders calcined at different temperatures. After calcining at 1000 °C, the gelcasts with different calcium dosage were almost converted into perovskite phase (Fig. 2a). Small peak shifts were found with the substitution of calcium. This may be attributed to the lattice parameter changes caused by the radius difference of the doping ions. It can also be seen that most perovskite phase forms at 800 °C (Fig. 2b), and only a small amount of carbonates and oxides remain. When the calcination temperature increases to 900 °C, the solid-state reaction results in the formation of perovskite phase with a corresponding decrease in carbonate and oxide phases. Pure LSCCF powders with perovskite structure are formed when the calcination temperature increases to 1000 °C. This indicates that pure perovskite phase can be obtained at a relatively low calcination temperature compared with the conventional solid-state reaction method [19]. When the calcination temperature further increases to 1100 °C, the samples retain perovskite structure, but diffraction peaks become sharper and narrower than those of 1000 °C, indicating grain growth of the calcined powders. Mean grain size calculated from XRD patterns, according to the Scherrer formula are 29.99 nm and 36.17 nm for the powders with $x = 0.2$ calcined at 1000 °C and 1100 °C, respectively. Fig. 3 shows TEM graphs of the calcined LSCCF powders. The powders are well-dispersed and have a narrow particle size distribution, and as calcination temperature increases, the powder becomes smooth and spherical. Fig. 3 also indicates that particle size of the LSCCF powder decreases with calcium dosage. While the powder with $x = 0.2$ has a mean particle size of about 200 nm, the powder with $x = 0.4$ only has a mean particle size of about 100 nm. The particle sized determined by TEM is bigger than the mean grain size determined by XRD, which can be ascribed to the polycrystalline structure of the particles.

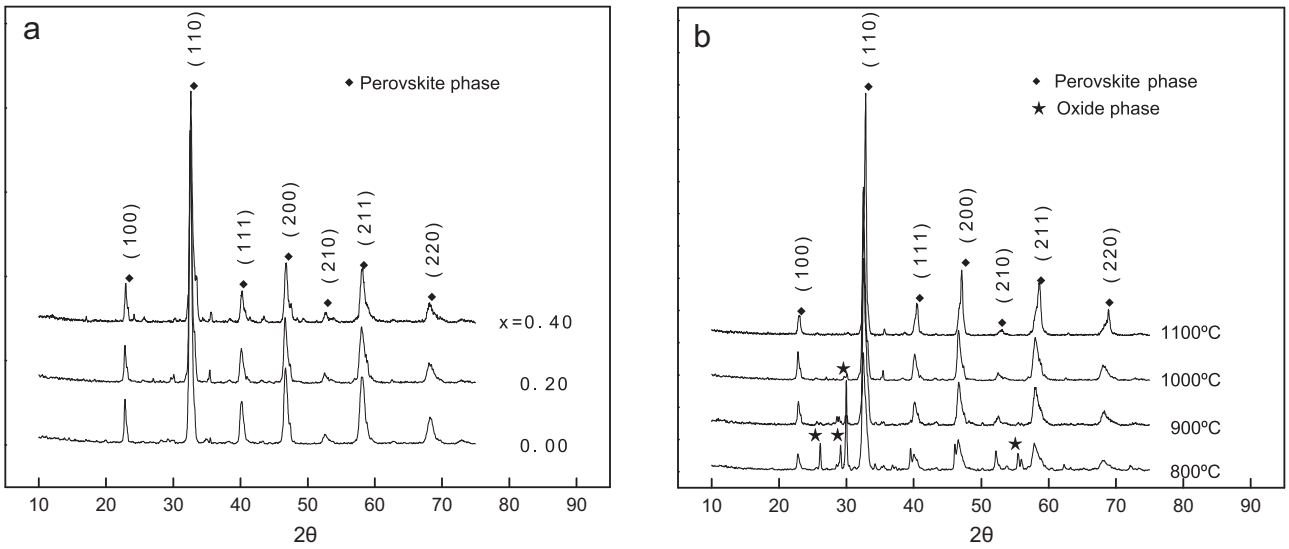

Fig. 2. XRD patterns of the calcined LSCCF powders: (a) powders with different Ca dosages calcined at 1000 °C and (b) powders ($x = 0.2$) calcined at different temperature.

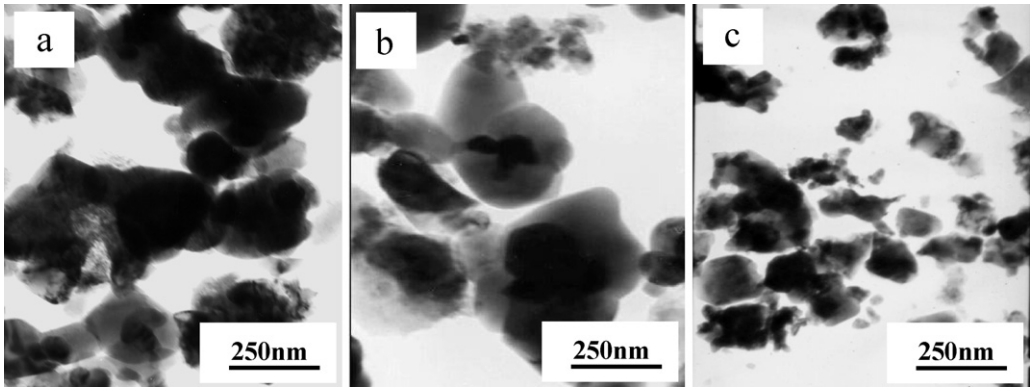

Fig. 3. TEM photos of the LSCCF powders: (a) $x = 0.2$, 1000 °C; (b) $x = 0.2$, 1100 °C and (c) $x = 0.4$, 1000 °C.

3.3. Porosity and microstructure of the sintered LSCCF samples

Fig. 4 shows porosity of the LSCCF samples sintered at different temperatures. Both total and open porosity of the samples decreases as sintering temperature increases. Fig. 4 also shows that the samples sintered at 1100 °C and 1150 °C have a total porosity above 20%, and in this case the open porosity is only slightly lower than the total porosity. This means that most pores are open (connected) when the total porosity of the LSCCF sample is above 20%. It can also been seen from Fig. 4 that calcium dosage has an

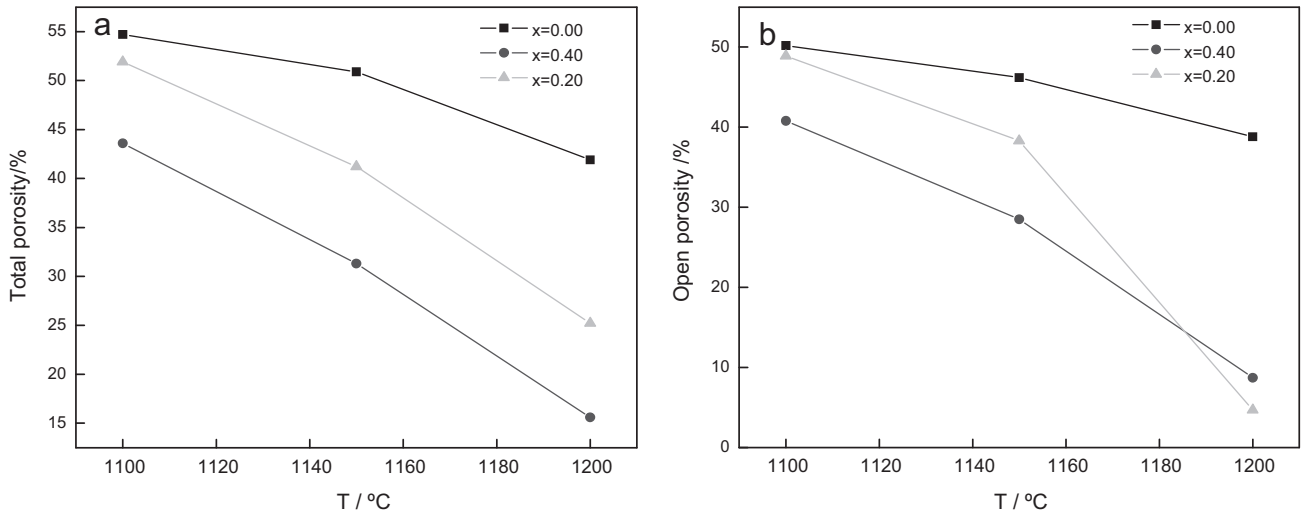

Fig. 4. Porosity of the LSCCF samples with different Ca dosages sintered at different temperature: (a) total porosity and (b) open porosity.

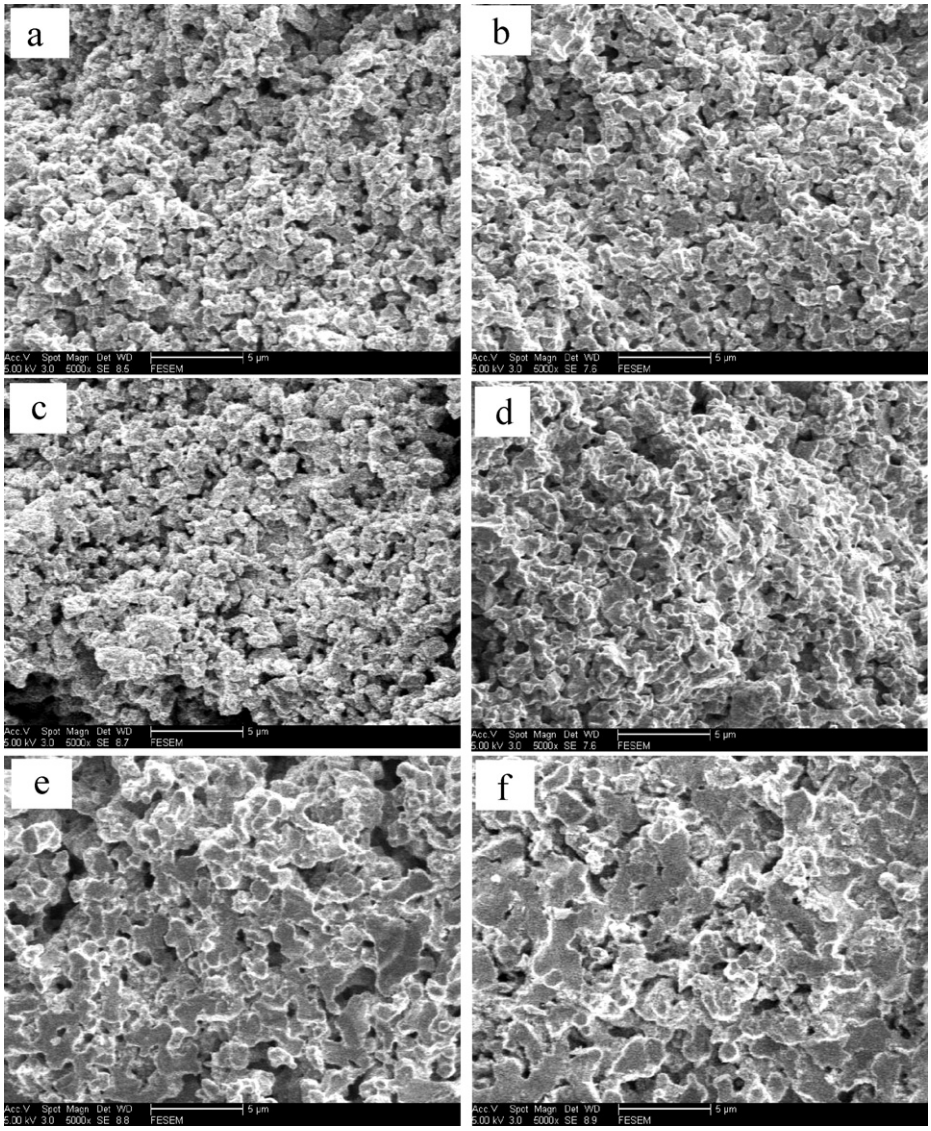

Fig. 5. SEM photographs of the sintered LSCCF samples: (a) $x = 0.0$, 1100 °C; (b) $x = 0.0$, 1150 °C; (c) $x = 0.2$, 1100 °C; (d) $x = 0.2$, 1150 °C; (e) $x = 0.4$, 1100 °C and (f) $x = 0.4$, 1150 °C.

obvious influence on the pore characteristics. When there is no calcium dosage ($x = 0.0$), the open porosity is 46.2%; but this value reduces to 38.3% and 28.5% for $x = 0.2$ and $x = 0.4$ respectively. It has been shown in Fig. 3 that particle size of the LSCCF powders decreases as calcium dosage increases, and the reduction of particle size can facilitate the sintering densification. Therefore, total and open porosity of the LSCCF samples decrease as calcium dosage increases.

Fig. 5 shows SEM micrographs of the LSCCF samples sintered at 1100 °C and 1150 °C with different calcium dosages. Fine grains and pores with homogenous distribution are also observed in Fig. 5, which is beneficial to the transmission of oxidation gas and to the increase of the area of the tripe phase boundary (TPB).However, The samples become dense as sintering temperature, as well as calcium dosage increases, and samples with $x = 0.4$ have higher density and bigger grain size than the others. This is consistent with the results shown in Fig. 4. Because the microstructure (pore characteristic) of the cathode plays an important role in transporting oxidation gases and in determining the three-phase zones during SOFC operation, the present work has shown that sintering temperature and composition of the cathode material should be properly designed to optimize the cathode performance of intermediate temperature solid oxide fuel cells.

3.4. Electrical conductivity of the sintered LSCCF samples

Fig. 6 shows Arrhenius plots of electrical conductivity of the LSCCF samples. The LSCCF material shows behaviors of ionic-electronic mixed conductors. In low temperature range, the electrical conductivity increases as testing temperature rises. This behavior is consistent with small polaron conduction (localized electronic carriers having a thermally activated mobility) [19]. In high temperature range, however, the electrical conductivity decreases as testing temperature increases. This may be ascribed to the formation and aggregation of oxygen vacancies in the LSCCF materials at relatively high temperature. In addition, the increase of intrinsic oxygen spillage and oxygen vacancy concentration facilitates the ionic compensation and weakens the small polaron conductivity, which also results in the deviation of $Ln\,(\sigma T)$ and T^{-1} in high temperature range.

The effects of calcium dosage on the electrical conductivity are also shown in Fig. 6. As calcium dosage increases, the

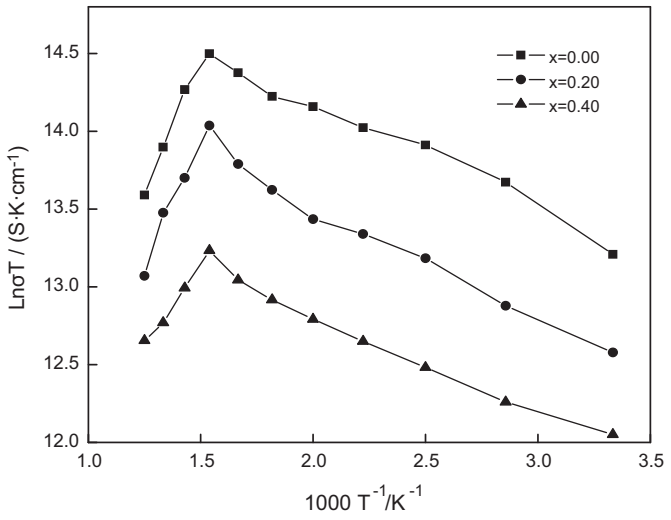

Fig. 6. Arrhenius plots of electrical conductivity of the LSCCF samples (sintered at 1100 °C) with different calcium dosages.

electrical conductivity decreases. Ca^{2+} has an ionic radius of 0.99 nm, smaller the ionic radii of Sr^{2+} (1.12 nm) and La^{3+} (1.06 nm), and when La^{3+} is partially substituted by Ca^{2+}, instead of Sr^{2+}, in the $La_{0.6}Sr_{0.4-x}Ca_xCo_{0.2}Fe_{0.8}O_3$ system, the vacancy concentration in the lattice structure is lowered. This leads to the reduction of ionic conductivity. Furthermore, the replacement of Sr^{2+} by Ca^{2+} also reduces the electrical conductivity of LSCCF materials due to the increase of the Co-O covalency and bandwidth [20]. On the other hand, as calcium dosage increases, porosity of the sintered LSCCF samples decreases and pore size increases (Figs. 4 and 5), which may results in the decrease of grain interfaces and vacancy concentration, and reduces the conductivity of the LSCCF materials.

3.5. Thermal expansion coefficient of the sintered LSCCF samples

Thermal expansion coefficient (TEC) of $La_{0.6}Sr_{0.4-x}Ca_xCo_{0.2}Fe_{0.8}O_3$ samples with different calcium dosage sintered at 1150 °C is shown in Fig. 7. TEC values of all samples increase as testing temperature rises, and when the testing temperature reaches a value (about 400 °C), the curves go up sharply.

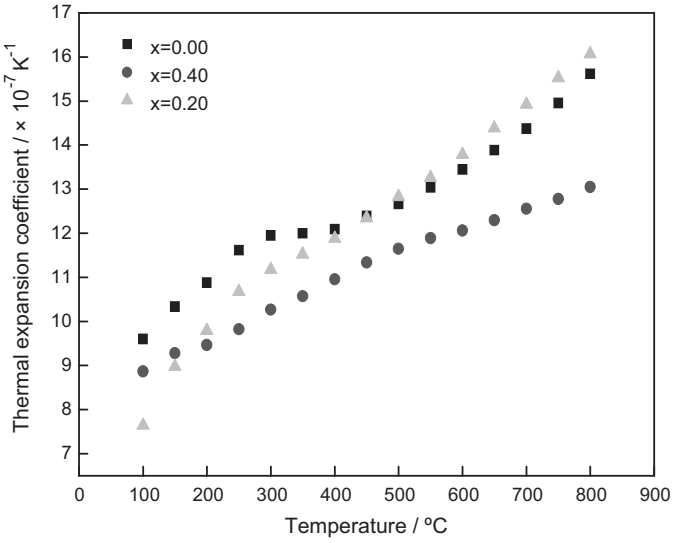

Fig. 7. Thermal expansion coefficients of the LSCCF samples with different calcium dosages sintered at 1150 °C.

This may be ascribed to the anomalistic lattice expansion caused by the formation of oxygen vacancies [21]. Fig. 7 also shows the effect of calcium doping on the thermal property of the LSCCF. Because TEC is mainly related to the bonding, when Sr^{2+} is partially replaced by Ca^{2+} in the LSCCF system, the bonding strength of Ca-O is higher than that of Sr-O. Therefore, the TEC values of the LSCCF materials decreases as calcium dosage. On the other hand, calcium doping increases sintered density of the LSCCF samples. This may also increase the thermal stabilization of the LSCCF materials, and reduces TEC values at same testing temperature.

4. Conclusions

$La_{0.6}Sr_{0.4-x}Ca_xCo_{0.2}Fe_{0.8}O_3$ (LSCCF, $x = 0$, 0.2, 0.4) powders were successfully synthesized by the gel-casting method using lanthana (La_2O_3), strontium carbonate ($SrCO_3$), cobalt oxide (Co_2O_3), calcium carbonate ($CaCO_3$) and iron oxide (Fe_2O_3) as starting materials. Perovskite LSCCF powders were obtained when the gelcasts were calcined at temperature above 1000 °C. Porosity of the LSCCF samples decreases as the sintering temperature increases. Calcium dosage and sintering temperature also greatly affect the conductivity and the thermal expansion coefficient of the LSCCF materials. While electrical conductivity of the LSCCF samples decreases as calcium dosage increases, the thermal expansion coefficient (TEC) shows a reverse change. $La_{0.6}Ca_{0.4}Co_{0.2}Fe_{0.8}O_3$ samples show the lowest TEC values. The present work has revealed that the LSCCF material may be a favorable candidate for cathode material of intermediate temperature solid oxide fuel cells.

Acknowledgments

This work is financially supported by the Natural Science Foundation of Anhui Province (contract No. 070414186), the Program of Science and Technology of Anhui Province (contract No. 2008AKKG0332), the Nippon Sheet Glass Foundation for Materials Science and Engineering (NSCF) and the Open Project Program of Key Laboratory of Low Dimensional Materials & Application Technology (Xiangtan University), Ministry of Education of China under contract No. DWKF0802.

References

[1] A. Zomorrodian, H. Salamati, Z. Lu, X. Chen, N. Wu, A. Ignatiev, Int. J. Hydrogen Energy 35 (2010) 12443–12448.
[2] S. Shahgaldi, Z. Yaakob, D.J. Khadem, M. Ahmadrezaei, W.R.W. Daud, J. Alloys Compd. 509 (2011) 9005–9009.
[3] M. Tsai, C. Chu, S. Lee, J. Alloys Compd. 489 (2010) 576–581.
[4] J.W. Yun, S.P. Yoon, S. Park, J. Han, S.W. Nam, T. Lim, J. Kim, Int. J. Hydrogen Energy 34 (2009) 9213–9219.
[5] B. Liu, Y. Zhang, J. Alloys Compd. 453 (2008) 418–422.
[6] C.J. Fu, Q.L. Liu, S.H. Chan, X.M. Ge, G. Pasciak, Int. J. Hydrogen Energy 35 (2010) 11200–11207.
[7] T. Huang, X. Shen, C. Chou, J. Power Sources 187 (2009) 348–355.
[8] J.H. Kim, Y.M. Park, H. Kim, J. Power Sources 196 (2011) 3544–3547.
[9] L. Sun, Q. Li, H. Zhao, L. Huo, J. Grenier, J. Power Sources 183 (2008) 43–48.
[10] H.W. Nie, T.-L. Wen, S.R. Wang, Y.S. Wang, U. Guth, V. Vashook, Solid State Ionics 177 (2006) 1929–1932.
[11] B.T. Dalslet, M. Søgaard, H.J.M. Bouwmeester, P.V. Hendriksen, Solid State Ionics 180 (2009) 1173–1182.
[12] B.T. Dalslet, M. Søgaard, P.V. Hendriksen, Solid State Ionics 180 (2009) 1050–1060.
[13] V. Vashook, D. Franke, J. Zosel, L. Vasylechko, M. Schmidt, U. Guth, J. Alloys Compd. 487 (2009) 577–584.
[14] X. Ding, Y. Liu, L. Gao, L. Guo, J. Alloys Compd. 458 (2008) 346–350.
[15] F. Zhang, T. Kato, M. Fuji, M. Takahashi, J. Eur. Ceram. Soc. 26 (2006) 667–671.
[16] S. Alkoy, H. Yanik, B. Yapar, Ceram. Int. 33 (2007) 389–394.
[17] M.R. Pillai, D. Gostovic, I. Kim, S.A. Barnett, J. Power Sources 163 (2007) 960–965.
[18] B. Chen, T. Zhang, J. Zhang, Q. Lin, D. Jiang, Ceram. Int. 34 (2008) 359–364.
[19] L. da Conceição, A.M. Silva, N.F.P. Ribeiro, M.M.V.M. Souza, Mater. Res. Bull. 46 (2011) 308–314.
[20] J. Xue, Y. Shen, T. He, Int. J. Hydrogen Energy 36 (2011) 6894–6898.
[21] J. Richter, P. Holtappels, T. Graule, L.J. Gauckler, Solid State Ionics 179 (2008) 2284–2289.